

Complexation characteristics of permethylated cycloinulohexaose, cycloinuloheptaose, and cycloinuloctaose with metal cations †

2 PERKIN

Motohiro Shizuma,^{*a} Yoshio Takai,^b Mishio Kawamura,^c Tokuji Takeda^a and Masami Sawada^{*b}

^a The Technochemistry Department, Osaka Municipal Technical Research Institute, Joto-ku, Osaka 536-8553, Japan

^b Materials Analysis Center, The Institute of Scientific and Industrial Research, Osaka University, Ibaraki, Osaka 567-0047, Japan

^c Department of Biology, Osaka Kyoiku University, Kashiwara, Osaka 583-8582, Japan

Received (in Cambridge, UK) 23rd March 2001, Accepted 4th June 2001

First published as an Advance Article on the web 29th June 2001

The host–guest complexation behavior of cyclic oligosaccharides, permethylated cycloinulohexaose **1**, permethylated cycloinuloheptaose **2**, and permethylated cycloinuloctaose **3** with metal cations has been characterized by means of UV-visible, NMR, and electrospray ionization (ESI) mass spectrometry. In the crystal state, the structures of **1**·K⁺, **1**·Rb⁺, and **1**·Cs⁺ were same as that of the **1**·Ba²⁺ complex which has a u-u-d-u-u-d (u = up, d = down) furanose ring arrangement for the plane of the crown ring moiety. The association constants (K_S) in THF and in [2H₆]acetone at 298 K were evaluated. The binding ability of host **1** with metal cations was of the same degree as that of calix[6]arene derivative **4** and much higher than those of hosts **2** and **3**. The thermodynamic parameters of the complexation of host **1** with metal cation in THF were determined, and it was suggested that the entropy change for the solvation of the metal cations was one of the important factors in the complexation equilibrium. It was clarified that the structure of the host **1**·K⁺ complex in solution at low temperature (furanose ring arrangement: u-d-u-d-u-d) was different from that in the crystal state (u-u-d-u-u-d arrangement) by the coalescence behavior in ¹H-NMR. The relative peak intensity of the complex ions of host **1** or **2** with two alkali metal ions in ESI mass spectrometry (in acetone) showed a correlation in the first order approximation with the ratio of the corresponding complex ion concentrations estimated from the K_S values.

Introduction

It is well-known that some kinds of peptides and natural ionophores such as monensin, valinomycin, *etc.*, play important roles as ion carriers and as ion channels in the typical metal ion-transport system which is one of the fundamental mechanisms for accumulation of energy, and the medium by which muscle is controlled, and information passed on in living systems.^{1–4} On the other hand, various hosts such as crown ethers,⁵ cryptands,⁶ spherands,⁷ cavitands,⁸ calixarenes,⁹ *etc.* have been synthesized and widely studied as artificial ion carriers. In particular, calix[4]arene derivatives have been reported to have high selectivity toward alkali metal ions (Na⁺–K⁺ = *ca.* 400 at 298 K in MeOH).¹⁰

Cyclofructans are one of the cyclic oligosaccharides and are structural isomers of cyclodextrins.¹¹ Cyclodextrins are cyclic oligomers composed of $\alpha(1\rightarrow4)$ linked D-glucopyranose units, while cyclofructans consist of $\beta(2\rightarrow1)$ linked D-fructofuranose units. Therefore, their structure and properties are quite different. Cyclofructans are expected to be a new carbohydrate type of ionophore because of the existence of the crown ether ring skeleton in the center of the molecules.¹² However, there have been few reports on the complexation of cyclofructans and their derivatives with metal cations as yet,^{13–15} and further development of this field has been expected.

In this paper, we report a further insight into the complex-

ation behavior of permethylated cycloinulohexaose **1**, permethylated cycloinuloheptaose **2**, and permethylated cycloinuloctaose **3** with metal cations.

Results

Solid ¹³C-NMR

The ¹³C-NMR spectra of host **1** in [2H]chloroform, host **1**·K⁺ complex (counter anion: picrate) and host **1**·Ba²⁺ complex (counter anion: SCN[−]) in the crystal state, at room temperature are shown in Fig. 1. In the solution state, 6 peaks of the fructofuranose moiety (C1–C6) and 3 peaks of the methoxy groups (3-OMe, 4-OMe and 6-OMe) were observed, respectively. In the solid state, each ¹³C-NMR peak in both of host **1**·K⁺ complex and host **1**·Ba²⁺ complex was observed as three peaks. The signals in solid ¹³C-NMR spectra of host **1**·Rb⁺ complex and host **1**·Cs⁺ complex were also observed as three split peaks, respectively.

UV-visible spectrometry

Bathochromic shifts of absorption maxima ($\Delta\lambda$ of λ_{\max}) of the picrate anion induced by adding a host to a metal picrate in THF at 298 K were observed (Fig. 2 and Table 1).¹⁶ The shifts induced by adding calix[6]arene derivatives **4** are also shown for comparison with permethylated cyclofructans.¹⁷ The association constants (K_S) of complexation between the host and a metal cation guest were then determined from the absorption changes at certain wavelengths at 298 K (Table 2). The thermodynamic parameters were estimated from K_S at various temperatures.¹⁸ In the case of host **1** with K⁺, Rb⁺, and

† Electronic supplementary information (ESI) available: a plot of log K_S for 1/T in the complexation of host **1** with K⁺ (Fig. S1), a typical ESI mass spectrum of the complex ions (Fig. S2), and a chromatographic chart of cyclofructans ($n=6-8$) (Fig. S3). See <http://www.rsc.org/suppdata/p2/b1/b102710g>

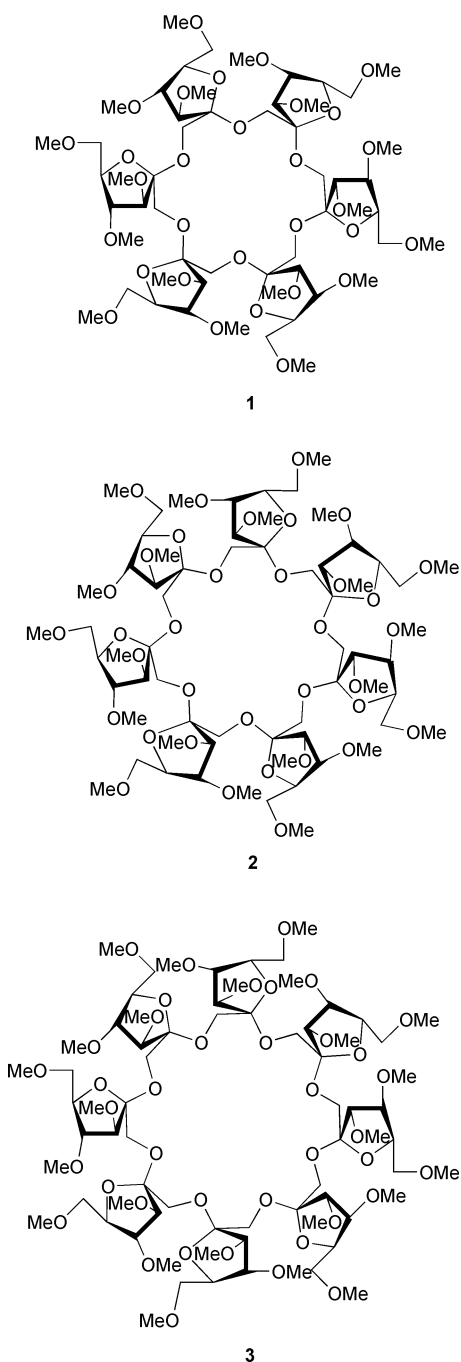


Table 1 Bathochromic shifts ($\Delta\lambda$ of λ_{\max} , nm) of the picrate anion probe by adding permethylated cyclodextrans **1**, **2** and **3** and calixarene derivative **4** in THF at 298 K

Guest cation	Host			
	1	2	3	4
Na ⁺	~5 ^a	1	0	6 (6 ^b)
K ⁺	24	~1	0	24 (25 ^b)
Rb ⁺	22	11	0	21
Cs ⁺	18	2	0	20 (20 ^b)
NH ₄ ⁺	~7 ^a	2		
Ba ²⁺	~3 ^a	0		

^a Isosbestic correlation disappeared, so we could not detect the exact $\Delta\lambda$. ^b Ref. 17 (at 303 K).

Cs⁺, large bathochromic shifts were observed. In the case of host **1** with Na⁺, a larger shift was observed by adding excess host **1**, but the isosbestic point disappeared. In the case of host **2** with Rb⁺, a clear bathochromic shift was observed. However,

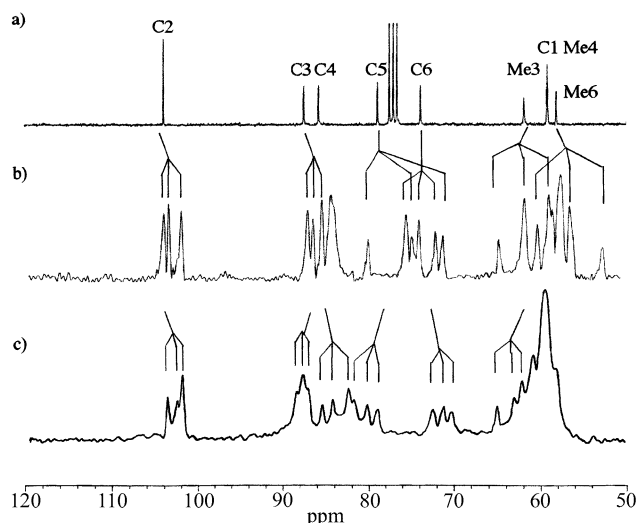


Fig. 1 A liquid ¹³C-NMR spectrum of host **1** and solid ¹³C-NMR spectra of host **1** complex with metal cations. (a) Host **1** in [²H]chloroform, (b) crystalline host **1**·K⁺ complex (counter anion: picrate), (c) host **1**·Ba²⁺ complex (counter anion: SCN⁻).

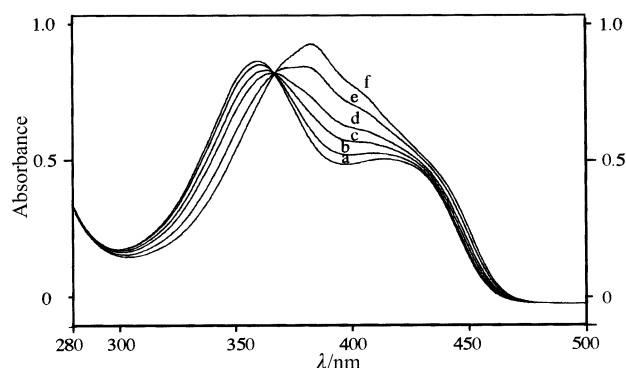


Fig. 2 UV-visible spectra of a 5.0×10^{-5} M THF solution of potassium picrate in the presence of different amounts of **1** at 298 K. Molar ratio of the host to metal picrate guest ($[H]/[G]$): (a) 0, (b) 0.3, (c) 0.7, (d) 1.4, (e) 2.7, (f) 7.0. Addition of variable amounts of **1** caused a bathochromic shift of λ_{\max} from 358 to 382 nm ($\Delta\lambda = 24$ nm).

for the other metal cations, only small shifts were observed. In the case of host **3**, no shifts were observed. The K_S ordering of host **1** with the metal picrates was $K^+ > Rb^+ > Cs^+ > Na^+$. The K_S value of host **2** with Rb⁺ was about 10² times smaller than that of host **1**. For the thermodynamic parameters, the ordering of the enthalpy (ΔH) and the entropy (ΔS) of host **1** was $K^+ > Rb^+ > Cs^+$ (Table 2).

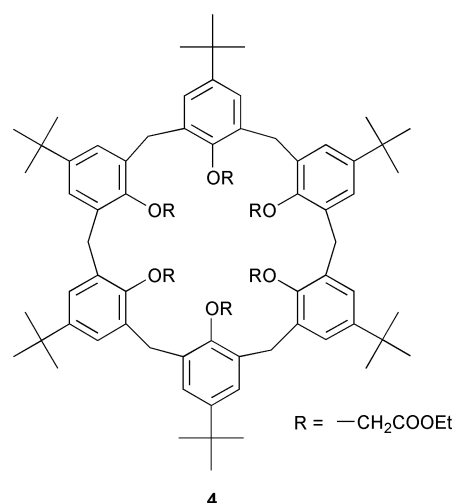


Table 2 $\text{Log}K_S$ and thermodynamic parameters for the complexation of host **1**, **2**, **4** and 18-crown-6 (18C6) with various metal cations (counter anion: picrate) in THF at 298 K.

Host	Cation	$\text{Log}K_S$	$\Delta G^\circ/\text{kcal mol}^{-1}$	$\Delta H^\circ/\text{kcal mol}^{-1}$	$T\Delta S^\circ/\text{kcal mol}^{-1}$
1	Na^+	3.25 ± 0.03			
1	K^+	4.34 ± 0.04	-6.0	-1.8	4.2
1	Rb^+	4.23 ± 0.03	-5.8	-3.4	2.4
1	Cs^+	4.03 ± 0.04	-5.6	-9.1	-3.3
2	Rb^+	2.71 ± 0.01	-4.6	-4.2	-0.3
4	K^+	4.20 ± 0.01^a			
18C6	Rb^+	5.12 ± 0.04^b			

^a $\text{Log}K_S = 4.13$ at 303 K (ref. 17). ^b At 303 K ($\Delta\lambda_{\text{max}} = 8$ nm).

Table 3 $\text{Log}K_S$ and $^1\text{H-NMR}$ induced shifts of permethylated cyclofructans (**1–3**) with metal cations (counter anion: SCN^-) in $[\text{D}_6]\text{acetone}$

Host	Guest	$\text{Log}K_S$	Low-field induced shift (ppm)										
			H-1	H-1'	H-3	H-4	H-6	H-6'	3-OMe	4-OMe	6-OMe		
1	Li^+	1.4 ± 0.1	(6) ^a	-0.21	0.02	0.04	0.17				0.12	0.09	0.05
1	Na^+	2.2 ± 0.1	(3)	-0.09	0.06	0.02	0.18				0.10	0.08	0.04
1	K^+	3.8 ± 0.0	(2)	-0.23	-0.01	0.05	0.02				0.16	0.10	0.05
1	Rb^+	3.6 ± 0.0	(3)								0.14	0.10	0.06
1	Cs^+	2.9 ± 0.0	(4)								0.08	0.06	0.03
1	Ca^{2+}	0.36 ± 0.02^b	(3)								0.08	0.07	0.04
1	Ba^{2+}	4.3	(1)	-0.09	-0.01	0.21	0.36				0.35	0.16	0.09
2	Na^+	1.1 ± 0.1^c	(4)								0.07	0.04	0.03
2	K^+	1.5 ± 0.1	(9)	-0.06	0.07	-0.03	0.11	0.07	0.07		0.10	0.06	0.04
2	Rb^+	2.0 ± 0.1	(6)			-0.04	0.07	0.07			0.09	0.05	0.03
2	Cs^+	1.9 ± 0.1	(8)	-0.05	0.04		0.05	0.03	0.03		0.03	0.02	0.01
2	Ba^{2+}	0.71 ± 0.06	(3)								0.07	0.05	0.06
3	Na^+	0.94 ± 0.06	(4)	0.23		-0.05					0.16	0.12	0.14
3	K^+	0.65 ± 0.07	(3)								0.19	0.14	0.19
3	Rb^+	1.0 ± 0.1	(3)								0.05	0.06	0.11
3	Cs^+	1.4 ± 0.1	(2)								0.01	0.02	0.01
3	Ba^{2+}	1.1 ± 0.0	(3)								0.28	0.18	0.18

^a Values in () are numbers of monitored peaks. ^b We can not remove completely crystal water by heating under vacuum. ^c The association constant of the **1** : **2** complex was estimated ($K_{S,12} = 0.1 \pm 0.03 \text{ M}^{-1}$).

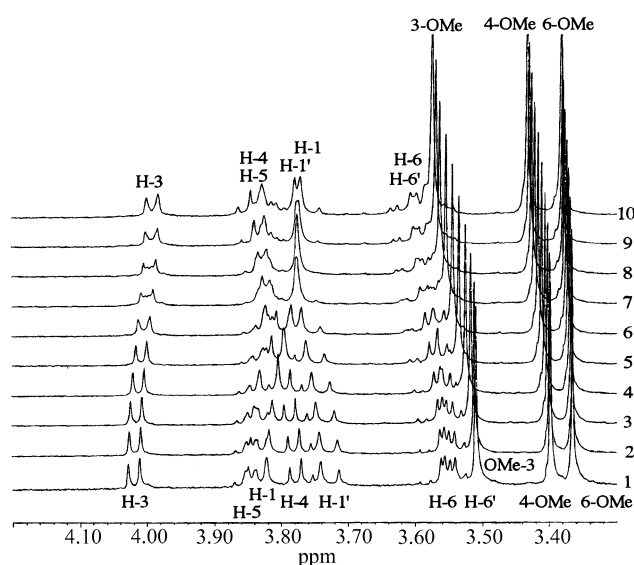


Fig. 3 $^1\text{H-NMR}$ (360 MHz) spectral changes of **2** with added Rb^+ (SCN^-) in $[\text{D}_6]\text{acetone}$ (298 K) ($[\text{H}]_0 = 0.726 \text{ mM}$). Ratio of concentration $[\text{H}]/[\text{G}]$: (1) 0, (2) 0.36, (3) 1.09, (4) 2.54, (5) 5.10, (6) 8.75, (7) 14.2, (8) 21.5, (9) 28.8, (10) 36.0.

NMR titration

The induced shifts of the $^1\text{H-NMR}$ peaks of the hosts in $[\text{D}_6]\text{acetone}$ at 298 K on adding metal cations (counter anion: SCN^-) were observed, and the K_S values were determined from the shifts (Fig. 3). The values are summarized in Table 3

including the values reported before.^{14b} The ordering of K_S of host **1** with metal cations was $\text{Ba}^{2+} > \text{K}^+ > \text{Rb}^+ > \text{Cs}^+ > \text{Na}^+ > \text{Li}^+ > \text{Ca}^{2+}$. In the case of host **2**, the ordering was $\text{Rb}^+ > \text{K}^+ > \text{Cs}^+ > \text{Na}^+ > \text{Ba}^{2+}$. In host **3**, the ordering was $\text{Cs}^+ > \text{Ba}^{2+} > \text{Rb}^+ > \text{K}^+ > \text{Na}^+$. In the case of hosts **1** and **2**, the downfield shifts of the three singlet signals of the OMe groups were observed, and the ordering of the downfield shifts was 3-OMe > 4-OMe > 6-OMe. For the ring protons, one of the two H-1 protons showed large upfield shifts. The H-4 protons showed large downfield shifts. For host **3**, no specific cation-induced shifts were observed.

Temperature-dependent $^1\text{H-NMR}$

$^1\text{H-NMR}$ spectra of the free host **1** or the complexes of the host **1** with metal cations (counter anion: SCN^-) were measured at various low temperatures in order to observe the coalescence of the proton peaks (Table 4). The mixture of solvents $[\text{D}_2]\text{chloroform}$ and $[\text{D}_2]\text{dichloromethane}$ was used because of the ease of treatment at low temperatures. The coalescence behavior of the proton peaks of host **1** was observed in the temperature range of 185 to 205 K, and the peaks split into two (Fig. 4). The number of splitting peaks suggests the symmetry of the molecule or the peaks, *etc.*, as reported before.^{14b} In the case of the complexes of host **1** with Na^+ , K^+ , and Cs^+ , the signals split into two. In the complex of the host **1** with Ba^{2+} , the peak was separated into three peaks. The activation free energy (ΔG_C^\ddagger) of the conformational interconversion was evaluated from the splitting width ($\Delta\nu$) and the coalescence temperature (T_C).¹⁹ The ordering of the ΔG_C^\ddagger was free host **1** < host **1**· Na^+ < host **1**· K^+ < host **1**· Ba^{2+} .

Table 4 Coalescence behavior and expected structure of host **1** and the complexes with metal cations (counter anion: SCN⁻) in temperature-dependent ¹H-NMR (360 MHz)^a

Guest	Number of separated peaks	Molecular symmetry	Furanose ring arrangement	<i>T_c</i> /K	ΔG_C^\ddagger /kcal mol ⁻¹
—	2	<i>C</i> ₃	u-d-u-d-u-d	185–205	9.2
Na ⁺	2	<i>C</i> ₃	u-d-u-d-u-d	205–220	10.4
K ⁺	2	<i>C</i> ₃	u-d-u-d-u-d	230–240	12.0
Cs ⁺	2	<i>C</i> ₃	u-d-u-d-u-d		
Ba ²⁺	3	<i>C</i> ₂	u-u-d-u-u-d	285–295	13.2

^a Solvent: [²H]chloroform–[²H₂]dichloromethane (v/v = 1 : 3). The concentration of complexes was estimated at about 1.63 mM. Activation free energy (ΔG_C^\ddagger) of the conformational interconversion was estimated by the modified Eyring equation depending on coalescence temperature (*T_c*) and separating width ($\Delta\nu$).

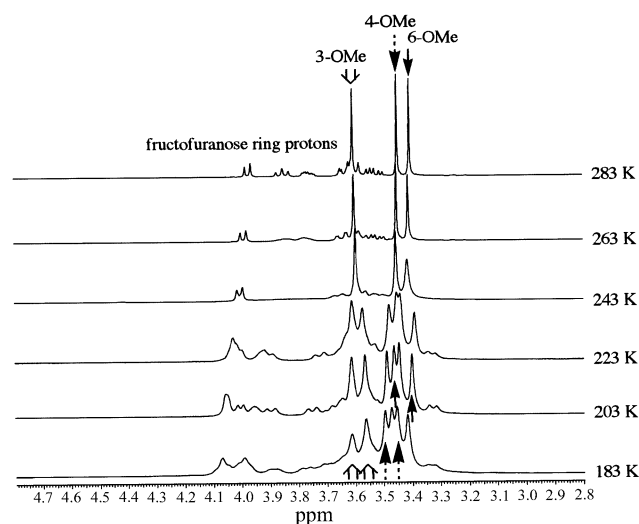


Fig. 4 Temperature-dependent ¹H-NMR (360 MHz) spectra of host **1** with K⁺ (SCN⁻) in [²H]chloroform–[²H₂]dichloromethane (v/v = 1 : 3). The concentration of complex was estimated at about 1.6 mM.

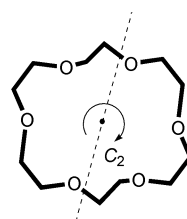
ESI mass spectrometry

ESI mass spectra of a three-component mixture in an acetone solution including the host and two kinds of metal cations (counter anion: SCN⁻) were measured. The relative peak intensity [$I(\text{host}\cdot\text{M})^+/I(\text{host}\cdot\text{K})^+$] of the complex ions of the host with alkali metal cation (M⁺) for the complex ion with K⁺ is shown in Table 5. For comparison between the binding ability of host **1** and that of host **2**, ESI mass spectra of a three-component mixture containing two hosts and K⁺ were also measured. In the case of host **1**, ordering of the relative peak intensity was K⁺ > Rb⁺ > Cs⁺ > Na⁺. For host **2**, the ordering was Rb⁺ > K⁺ > Cs⁺ > Na⁺. Compared with complex ions with K⁺, the peak intensity of the complex ions of host **1** was larger than that of host **2**.

Discussion

Structure of crystalline complexes

The crystalline host **1**·Ba²⁺ complex (counter anion: SCN⁻) had been already analyzed by means of X-ray crystallography.^{14b} In the complex, the barium ion is not located in the center of the 18-crown-6 ring skeleton but in the binding site consisting of the six oxygens of the crown ether ring skeleton and the four oxygens of the 3-OMe groups. Four fructofuranose rings which bind to the cation were above the crown ring plane, and two furanose rings were below the ring plane. The furanose ring arrangement is u-u-d-u-u-d (u = up, d = down) for the crown ring plane. The conformation of the crown ring skeleton was the twist boat type, and the arrangement of the –O–C–C–O– torsion angles was *g*⁺*g*⁺*g*⁺*g*⁺*g*⁺*g*⁺.²⁰ The complex has a *C*₂ symmetry axis (Fig. 5). Therefore, the crystalline complex has three stereochemically different fructo-



Conformation arrangement of 18-crown-6 ring moiety: *g*⁺*g*⁺*g*⁺*g*⁺*g*⁺*g*⁺

Fig. 5 Conformation of 18-crown-6 ring moiety in crystalline host **1**·Ba²⁺ complex.

Table 5 Relative peak intensity of the complex ions of permethylated cyclofructans (**1**, **2**) with metal cations (counter anion: SCN⁻) in electrospray ionization (ESI) mass spectrometry

Host	Metal cation 1	Metal cation 2	$I(\text{host}\cdot\text{M})^+/I(\text{host}\cdot\text{K})^+$ ^a
1	Na ⁺	K ⁺	14
1	Rb ⁺	K ⁺	66
1	Cs ⁺	K ⁺	26
2	Na ⁺	K ⁺	81
2	Rb ⁺	K ⁺	122
2	Cs ⁺	K ⁺	52

^a All values were normalized as $I(\text{host}\cdot\text{K})^+ = 100$ except *b*. ^b The value was normalized as $I(\text{host}\cdot\text{K})^+ = 100$.

Guest	Host 1	Host 2	$I(\text{host}\cdot\text{2}\cdot\text{K})^+/I(\text{host}\cdot\text{1}\cdot\text{K})^+$
K ⁺	1	2	11 ^b

furanose moieties in six furanose units. This fact accounts for the results of solid ¹³C-NMR. The solid ¹³C-NMR spectra of host **1**·K⁺, host **1**·Rb⁺, host **1**·Cs⁺ complexes are similar to that of host **1**·Ba²⁺ complex. Thus, the solid NMR spectra suggest that these complexes have a *C*₂ symmetry axis in the crystal state. Although in the case of the crystalline complexes of host **1** with K⁺, Rb⁺ and Cs⁺ (counter anion: picrate), a few parts of the methoxy groups on the edge and others have not been solved yet, it was found that the conformation of the 18-crown-6 ring skeleton was the twist-boat type (*g*⁺*g*⁺*g*⁺*g*⁺*g*⁺) and the four fructofuranose rings were located on the ring plane (u-u-d-u-u-d arrangement).²¹ In the crystalline complexes of host **1** with a series of metal cations (K⁺, Rb⁺, Cs⁺ and Ba²⁺), host **1** has a regular conformation (see later).

Distance between metal cation and picrate

With the change in distance between the oxygen and potassium ions in the potassium picrate model, whose structure was optimized by the PM3 semiempirical molecular orbital method,²² the UV-visible spectra of the modified potassium picrate were simulated by means of the ZINDO calculation method.²³ The difference ($\Delta\lambda$) between the wavelength ($\lambda_{\text{max}0}$) of the absorption maxima in the initial optimized structure and the wavelength

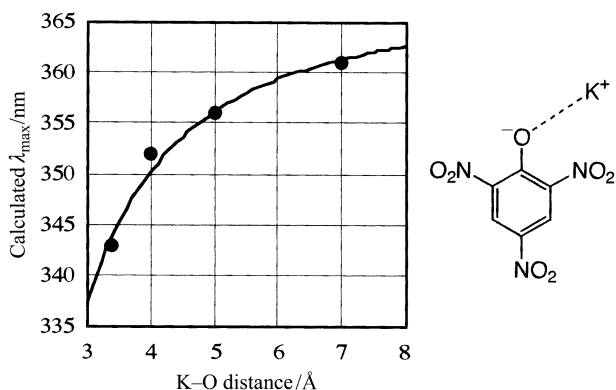


Fig. 6 Bathochromic shifts (BS, $\Delta\lambda$) of λ_{\max} of picrate anion vs. K–O distance (r). The line is the fitting curve of $BS = -k(1/r^2)$ (where k is a constant). The bathochromic shifts were calculated by ZINDO simulation.

λ_{\max} was plotted against the K^+ –O distance (Fig. 6). The longer the K^+ –O distance, the larger the bathochromic shift. It is deduced from the plot curve that the K^+ –O distance is *ca.* 7 Å because the experimental bathochromic shift is 24 nm. Therefore, it is suggested that the potassium picrate becomes a completely separated ion pair by the complexation with host **1** in THF.

Binding ability with metal cations

The binding ability of host **1** was very high in comparison with hosts **2** and **3**. The binding ability of host **1** was approximately as high as that of host **4** in THF. The $\log K_S$ value in THF at 298 K is linearly correlated with $\log K_S$ in $[^2H_6]$ acetone at 298 K. It is then suggested that difference between the counter anions (SCN^- or picrate) is negligible. The alkali metal cation-selectivity of host **1** ($K^+ > Rb^+ > Cs^+ > Na^+$) is different from the selectivity of host **4** ($Cs^+ > K^+ > Na^+$), and the difference is assumed to be the difference in flexibility of the binding cavities in the hosts. The binding cavity of host **1** consists of the 18-crown-6 ring skeleton and the 3-OMe groups of furanose rings spiro-anellated on the crown ring skeleton. On the other hand, the cavity of host **4** consists of phenol oxygens and carbonyl oxygens of the ethoxycarbonylmethyl moiety. The former would be more rigid than the latter. Host **1** then showed a clear selectivity for metal cation size. On the other hand, host **4** can change the cavity size flexibly according to the metal cation size, so that it showed higher binding ability to all alkali metal cations.

Correlation between metal cation selectivity and cavity size of hosts

From the correlation between the alkali metal ion radius and the K_S values, the cations having the highest K_S values of host **1**, host **2**, and host **3** among the alkali metal series (in $[^2H_6]$ acetone) have the same selectivity as the corresponding benzo crown ether series (in chloroform) (Fig. 7).²⁴ Characteristically, the larger the ring size of the permethylated cyclofructan series, the lower the binding ability. It is suggested that the binding sites of the hosts do not consist of only the crown ether ring skeleton but also the oxygens of the furanose rings in solution.

Thermodynamics

The contribution of the entropy factor (ΔS) to the free energy (ΔG) of the complexation equilibrium of host **1** with metal cations was large. In the case of host **1** with K^+ and Rb^+ , $\Delta H < 0$, $\Delta S > 0$, as in the case of cryptand[2.2.1] with alkali or alkaline earth ions such as Na^+ , K^+ and Mg^{2+} in water.²⁵ In general, the entropy is reduced in an intermolecular association system. However, because cryptands are cage-like structures,

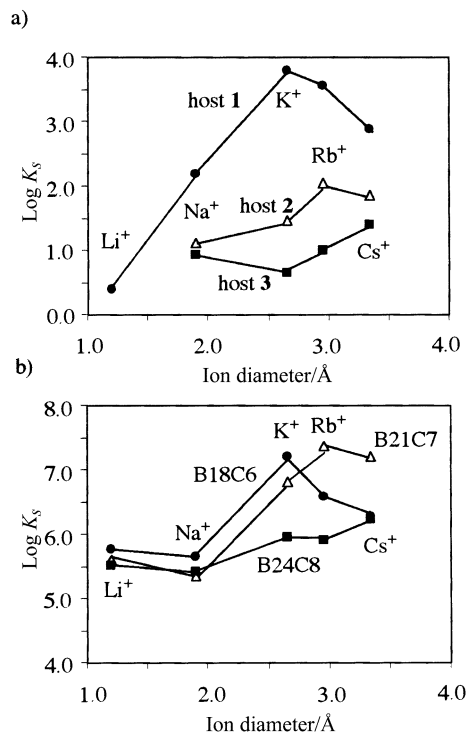


Fig. 7 $\log K_S$ vs. cation radius plots for the complexation of (a) permethylated cyclofructans (in $[^2H_6]$ acetone) or (b) benzo crown ethers (in chloroform) with alkali metal cations. B18C6 = benzo-18-crown-6, B21C7 = benzo-21-crown-7, B24C8 = benzo-24-crown-8.

the solvent around the metal cations would be completely torn off in the complexation with the cryptands. Therefore, in this case, the enhancement of entropy due to desolvation becomes large. This increase in the entropy negates the reduction in the entropy due to the association. The X-ray crystal structure of the complexes of host **1** with metal cations clearly shows that the cations are completely encapsulated within the cavity of the host. Therefore, it appears reasonable that the complexation of host **1** shows the entropy change (ΔS) as that of the cryptands. The ordering of the solvation affinity was $K^+ > Rb^+ > Cs^+$.²⁶ The ordering of the obtained $-T\Delta S$ was in good agreement with the solvent affinity. In the complexation with K^+ and Cs^+ , from a large negative ΔH , the distortion of host **1** seems to be larger in the former case probably because K^+ is smaller than Cs^+ . Host **1** seems to form a complex with Cs^+ with less stress.

Relationship between bathochromic shift and $\log K_S$

For host **1** and 18-crown-6, $\log K_S$ is plotted against the bathochromic shifts (Fig. 8). Host **1** with Na^+ , K^+ , Rb^+ , and Cs^+ shows a linear relation. Linearity is observed for 18-crown-6 with K^+ , Rb^+ , and Cs^+ , but not with Na^+ .²⁷ The magnitude of the bathochromic shifts depends on the average distance between the metal cation and the picrate anion. In the complexes of 18-crown-6 with K^+ , Rb^+ , and Cs^+ , the arrangements of $-O-C-C-O-$ torsion angles in the crown rings are represented by $g^+g^-g^+g^-g^+g^-$.²⁸ The arrangement is $g^+g^-g^+g^-g^+g^-$ in the complex with Na^+ .²⁹ The complexes of flexible host **4** are assumed to be different structures depending on the metal cation species. Shinkai *et al.* reported that there is no linearity between the bathochromic shifts and $\log K_S$ in the case of host **4** with alkali metal ions.¹⁷

Binding points between hosts and guests in solution

Induced shifts in the 1H -NMR peaks of host **1** by adding the present metal cations showed the following features. In the two types of H1 and H1' in the crown ring skeleton, high-field shift and low-field shift were observed. Among the three types of the OMe protons, the largest shifts were observed on the 3-OMe

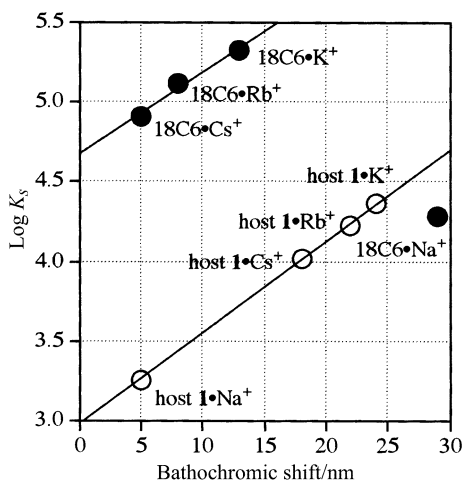


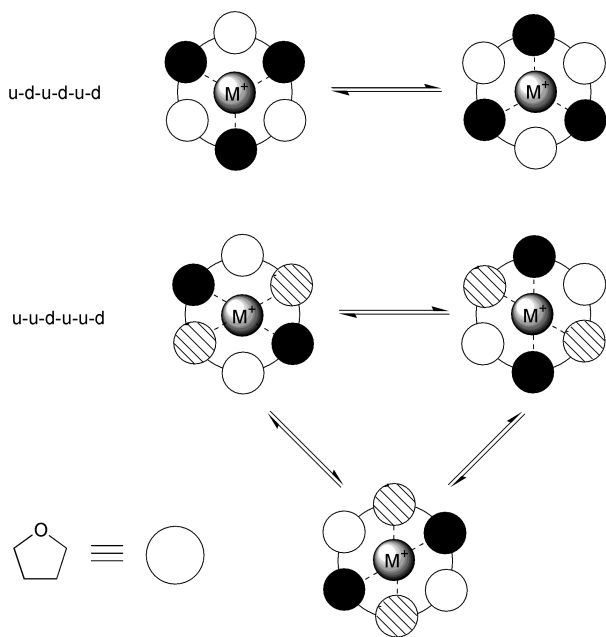
Fig. 8 $\log K_S$ vs. bathochromic shift plots for the complexation of host **1** (○) and 18-crown-6 (18C6) (●). Data for the host **1** series are determined in tetrahydrofuran. Data for 18C6•Na⁺, 18C6•K⁺, and 18C6•Cs⁺ are from ref. 24.

protons, a larger low-field shift on H-4, which is located *cis* to 3-OMe, and the oxygens of the 3-OMe groups are then believed to be coordinated to metal cations. These features were also observed in host **2**. In solution, host **1** and host **2** would form complexes with metal cations at binding points including the oxygens in the crown ring skeleton and the oxygens of the 3-OMe groups in the fructofuranose rings.

Fructofuranose ring arrangement of complexes in solution at low temperature

The activation free energy change (ΔG_C^\ddagger) estimated from coalescence behavior of the signals in temperature-dependent ¹H-NMR is assumed to involve an intramolecular conformation change in host **1** or its complexes as shown in Scheme 1. If

Expected furanose ring arrangement



Scheme 1

the binding ability between a host and a guest is high, it is expected that ΔG_C^\ddagger is larger because of controlled conformation inversion. Indeed, the ordering of ΔG_C^\ddagger agrees well with that of K_S . The two peaks (integration 1 : 1) of complexes of host **1** with Na⁺, K⁺ and Cs⁺ at low temperature would result

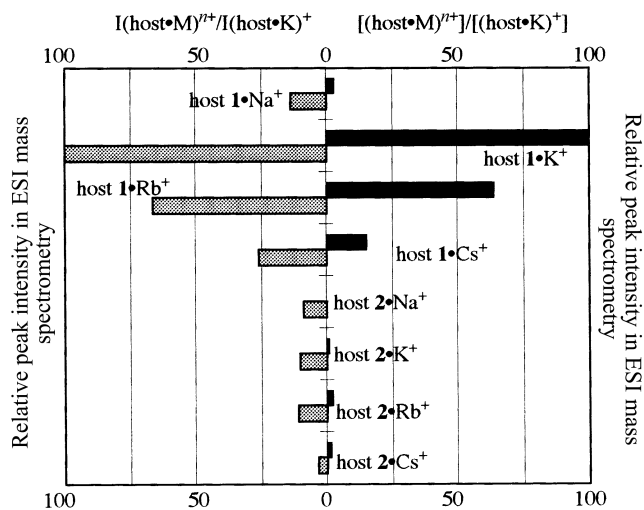


Fig. 9 Comparison of complex ion peak intensities in ESIMS and concentration ratio of complex ions calculated from K_S values in [²H₆]acetone at 298 K.

from the u-furanose rings and the d-furanose rings, respectively. Therefore, a possible complex structure in solution at low temperature may be expected to have C₃ symmetry and u-d-u-d-u-d furanose rings arrangement as in the crystalline structure of cyclinulohexaose (Table 4).¹² The structure of the host **1**•Ba²⁺ complex, which shows the highest binding ability in this series, may be expected to have C₂ symmetry (furanose ring arrangement: u-u-d-u-u-d) in good agreement with the result of the X-ray crystal structure analysis.

In our previous report, the charge induced shifts of host **1** were estimated on the basis of induced-shift differences in the ¹H-NMR spectra of the K⁺ and Ba²⁺ complexes at room temperature.^{14b} As indicated by Immel and Lichtenhaler,³⁰ the estimation of the charge-induced shift is valid only if both complexes exhibit identical or similar conformations in a strict sense. From the obtained linear relationship between bathochromic shift and $\log K_S$, this seems to be true at room temperature for a qualitative level. Considering the symmetry of the host–metal complexes in solution at low temperatures, the evaluation might not be quantitatively suitable for this system.

Relative peak intensity in ESI mass spectrometry

The relative peak intensity of the complex ions of host **1** and host **2** with a given alkali metal ion observed in ESI mass spectra is plotted against the ratio of the complex concentration estimated from K_S in [²H₆]acetone at 25 °C. The relative intensity is in agreement with the ratio of the concentration, especially in host **1** (Fig. 9). So far, it has been reported that the relative peak intensity in ESI mass spectrometry reflects the ratio of the complex concentration, in the case of crown ethers and cryptands with metal cations,³¹ and metal cation selectivity of various artificial ionophores studied in detail using ESI mass spectrometry under controlled conditions.³² The peak intensity in ESI mass spectra depends on various factors such as charges of ions, solvents, counter ions, and ionization conditions (accelerating cone voltage, capillary temperature, *etc.*). Although it is also reported that, in the case of modified crown ethers with alkylammonium ions, the relative intensity differs from the concentration ratio in solution.³³ Generally, the transferability of the metal ions to the gas phase from the liquid phase largely depends on the kind of cations because of the differences in the solvation effect.³⁴ Herein, acetone and thiocyanate were also used in order to estimate K_S values in solution as solvent and counter anion, respectively. However, under our conditions, we found good agreement between the relative intensity and the concentration ratio in solution, suggesting

that there are few transferability differences of the present complex ion. For complex ions consisting of metal cations with a host, which is similar to solvent molecules in solvation, the transferability factors may be leveled off to the same extent as the free metal cations.

Summary

The binding ability of host **1** with metal cations is relatively large compared to that of host **2** and host **3** in [²H₆]acetone. Unlike host **4**, which shows approximately the same binding ability in THF, host **1** was suggested to complex rather rigidly with a series of alkali metal cations in solution. In the case of host **1**·K⁺, host **1**·Rb⁺, and host **1**·Cs⁺ complexes, the liquid NMR spectrometrically deduced structure (furanose ring arrangement: u-d-u-d-u-d) at low temperature is clearly different from the crystalline structure (u-u-d-u-u-d) by the solid NMR.³⁵

Properties and structures of cyclofructan complexations have been studied and deduced by means of various spectral experiments and molecular simulations. Recently, the chiral discrimination ability of the permethylated cyclofructans toward amino acid derivatives has appeared.³⁶ Further study of these cyclic oligosaccharides will be continued to develop them as a new, interesting class of ionophore.

Experimental

Materials

Permethylated cyclofructans (1, 2, and 3). Free cyclofructans (hydroxy type) were isolated from a cyclic oligomer mixture (*n* = 6–8) obtained by enzyme reaction (Mitsubishi Kagaku Co.) using chromatography with an eluent of water through a column (size, Ø 25 × 350 mm (Ca) and Ø 25 × 550 mm (K)) filled with cation exchange resin (Dowex AG-50W) calcium and potassium forms under medium pressure (*ca.* 3.5 kgf cm⁻², flow 1.0 mL min⁻¹). The ordering of the retention time was octamer, heptamer and hexamer and they were obtained in the amounts of 7.8, 18.9 and 65.5 mg, respectively, from 100 mg of the mixture. The isolated cyclofructans were permethylated by the Hakomori method.³⁷ The products were identified by mp, FABMS, NMR, FT-IR, and elemental analyses.

Permethylated cycloinuloctaose (3). Under nitrogen gas flow, a dry DMSO solution of dry crude cycloinuloctaose 270 mg (0.21 mmol) was added to a stirred DMSO solution of dimethyl sulfinyl carbanion (*ca.* 12 mmol), which was prepared from NaH and dry DMSO, and was stirred for 4 h at room temperature. The reaction mixture was cooled in an ice bath, methyl iodide 2.7 mL (43.3 mmol) was added dropwise at *ca.* 10 °C, and stirred at room temperature overnight. To the reaction mixture was added dichloromethane, the organic layer was washed with aq. Na₂S₂O₃ and water, and the organic layer was dried over anhydrous MgSO₄ overnight. After filtration, the solution was evaporated *in vacuo* to give a residue that was purified by liquid column chromatography [filler, silica gel 60, Merck; eluted solvent, methanol–benzene = 1 : 8 (v/v)], and recrystallized from dichloromethane–petroleum ether to give 168 mg. The obtained white powder 110 mg was purified by preparative gel-permeation liquid chromatography (eluted solvent, chloroform) and recrystallized from dichloromethane–petroleum ether to yield **3** (50 mg, 15 %): colorless powder, mp 128–133 °C; ¹H-NMR (270 MHz, CDCl₃) δ (ppm) 4.08 (d, 8H, ³J_{3,4} = 7.1 Hz, H-3), 3.83 (m, 8H, H-5), 3.71 (d, 8H, ²J_{1,1'} = 10.0 Hz, H-1), 3.71 (dd, 8H, ³J_{3,4} = 6.9 Hz, H-4), 3.56 (m, 24H, H-1', H-6, H-6'), 3.48 (s, 24H, -CH₃), 3.43 (s, 24H, -CH₃), 3.39 (s, 24H, -CH₃) from TMS; FT-IR (KBr-disk) 1121, 1101, 1073 (ether CO) cm⁻¹; FABMS (*m/z*) 1671 (M + K)⁺; Anal. Calcd. for C₇₂H₁₀₈O₄₀: C, 52.93; H, 7.90. Found: C, 52.96; H, 7.91.

p-*tert*-Butylcalix[6]arene ester **4** was prepared by adding ethyl bromoacetate to a slurry of a commercial *p*-*tert*-calix[6]arene (Tokyo Kasei. Co.) and anhydrous potassium carbonate in acetone at room temperature³⁸ and identified by mp, ¹H-NMR and FT-IR. Commercial 18-crown-6 was used without purification (Aldrich).

Metal picrates were prepared by a neutralization reaction of picric acid and metal hydroxide in methanol and recrystallized in water.³⁹ The products were dried *in vacuo* for 5–10 h at 100 °C and used in UV-visible titration experiments. The metal picrates were identified by elemental analysis.

Metal thiocyanates were used without purification of commercial reagents which were dried under vacuum at 100 °C overnight (Na and Ca salts, Wako Co.; Li, K, Cs, and Ba salts, Kishida Chemical Co.). RbSCN was prepared by anion exchange through a liquid chromatographic column (anion exchange resin, Dowex AG1-X2 SCN form; water) from metal chloride (Wako Co.). Their formation was identified by atomic absorption analysis (Rb and Na) and ion chromatography (Cl⁻ and SCN⁻). The products were dried *in vacuo* at 80 °C before the experiment.

General

Solid ¹³C-NMR (70 MHz) spectra were taken with a JEOL EX-270 spectrometer. UV-visible spectra were taken with a Hitachi U-3410 UV spectrometer. ¹H-NMR (360 MHz) and ¹³C-NMR (90 MHz) spectra were taken with a Bruker AM400 spectrometer. TMS was used as the internal standard. ESI mass spectra were measured by using a Finnigan TSQ7000.

Liquid column chromatography for the isolation and the purification of cyclofructans was carried out on a Yamazen LC apparatus with an RI detector under appropriate medium pressure. Gel-permeation liquid chromatography was performed using a LC-09 (Nihon Bunseki Kougyou Co.) with an RI detector. The compounds used were identified with the following methods. Melting points were measured with a Yanaco micro melting point apparatus. ¹H-NMR (270 MHz) spectra were taken with a JEOL EX-270 spectrometer. FT-IR spectra were taken with an Analect RFX-65 or a Shimadzu FT-IR 8100 spectrometer. FAB mass spectra were taken with a JEOL JMS-600 (NBA matrix). Elemental analyses were performed using a Perkin-Elmer 2400. Ion chromatographic analyses were performed using a Dionex QIC analyzer. Atomic absorption analysis data were taken with a Dainiseikosha SAS/727.

Solid ¹³C-NMR

The crystalline structures of **1**·K⁺ (picrate) complex, **1**·Rb⁺ (picrate) complex, **1**·Cs⁺ (picrate) complex, and the **1**·Ba²⁺ (SCN⁻)₂ complex were analyzed using the solid ¹³C-NMR as follows. An aqueous solution of **1** with an excess amount of metal cation was allowed to evaporate slowly. The obtained single crystals were powdered by a mortar and about 100 mg of the powder was used for the solid ¹³C-NMR measurement. The single crystals were not suitable for X-ray crystallography because of their instability in air. A cross-polarization magic angle spinning (CPMAS) pulse sequence was applied. The spin ratio of the samples was about 6000 kHz. Adamantane was used as an indirect reference (chemical shift of the methyne carbon peaks: δ = 37.8 ppm).

MO calculation

The relationship between the bathochromic shift in UV-visible spectra and the cation–anion distance of potassium picrate was estimated with ZINDO calculation software in the CAChe work system (CAChe Scientific, Inc.). The initial structure of potassium picrate was obtained from the PM3 optimization in MOPAC (ver. 94. 10). Only the K–O distance in the fixed model

was changed ranging from 3.27 to 15 Å and the simulation of the configuration interaction in a ZINDO (parameter, INDO/1; SCF type, RHF; C. I. level, 8) at each K–O distance gave an electronic spectral pattern, *i.e.*, λ_{\max} in UV-visible. A plot of the K–O distance (r) vs. bathochromic shifts (BS) demonstrated the relationship of $BS = -k(1/r^2)$ (where k is a constant) that suggested a principal contribution of the electrostatic effect to the bathochromic shifts.

UV-visible experiments

The bathochromic shifts ($\Delta\lambda$) of λ_{\max} of a given metal picrate caused by adding hosts (1–4) in THF were determined as follows. Permethylated cyclofructans were gradually added to a *ca.* 5×10^{-5} M THF solution of metal picrate stirred magnetically in a UV cell until no shift was observed or until the isosbestic relationship disappeared. A new λ_{\max} was then determined from the UV-visible spectra. Commercial THF (spectrophotometric grade, Dojin Co.) was used without purification.

The K_S values of **1** and **2** with metal picrate were determined at constant temperature in THF. To maintain the temperature of the UV cell, water regulated at that temperature in a NESLAB endocal refrigerated circulating bath was allowed to flow into a circulating cell holder.

For a typical example, the case of host **1** with K^+ (picrate) at 18 °C: to 3 mL of a 4.43×10^{-5} M potassium picrate solution in THF was added A_{part} of a 3.17×10^{-2} M host **1** solution in THF ($A_{\text{part}} = 1, 2, 4, 8, 15, 30 \mu\text{L}$, thus $A_{\text{total}} = 60 \mu\text{L}$), and the UV-visible spectra of these solutions were measured. These concentration ratios $[H]/[G]$ of the host and the guest after the addition amounted to 0.239, 0.717, 1.67, 3.59, 8.26, and 14.3, respectively. The K_S values were determined using typical non-linear methods (1:1 simulation). The calculated K_S values were $2.69 \times 10^4 \text{ M}^{-1}$ (382 nm), $2.68 \times 10^4 \text{ M}^{-1}$ (394 nm), and $2.69 \times 10^4 \text{ M}^{-1}$ (400 nm). The averaged value was $(2.69 \pm 0.01) \times 10^4 \text{ M}^{-1}$.

Thermodynamic parameters were estimated from the linear relationship between $\log K_S$ measured at various temperatures and the reciprocal of the temperature ($1/T$). The slope and the intercept of the linear relationship fitted by least squares methods were estimated as ΔH and ΔS , respectively.

The UV and visible sources were D₂ and W lamps. The scan range was 280–500 nm and the scan speed was 120 nm min^{-1} . All temperatures in the UV cell were measured using a thermometer (thermocouple type, TAKARA thermistor instruments Co., D226).

¹H-NMR experiments

¹H-NMR spectra were measured using the ¹H-NMR titration technique reported before.¹⁴ Commercial [²H₆]acetone (Aldrich, 99.5 atom% D) was used as a solvent without purification. The K_S values of complexation equilibrium between the permethylated cyclofructans and metal thiocyanate at 25 °C (298 K) were determined by the following procedure. To an NMR tube containing a 0.5 mL [²H₆]acetone solution of permethylated cyclofructan of which the exact concentration was known was added dropwise a [²H₆]acetone solution of metal thiocyanate, whose concentration was exactly prepared, and ¹H-NMR spectra were measured in order. To maintain the sample solution at a constant temperature, the NMR tube was kept on the probe, which was maintained at 25 °C (298 K), for over 15 min before measurement of the NMR spectra. The averages of the K_S values estimated from the concentration ratio $[G]/[H]$ and the corresponding shifts of the resulting proton peaks (1–9 peaks) were adopted. The K_S values were calculated using a general non linear method.¹⁴

The stoichiometry of host **1** with all alkali metal ions and host **2** with rubidium ion were confirmed to be 1 : 1 complexes by the Job's plot.⁴¹ In the case of host **2** with NaSCN, the behavior of ¹H-NMR induced-shifts suggested the formation

of a 1 : 2 (**2**–metal) complex. The $K_{S1:1}$ and $K_{S1:2}$ values were estimated by a non-linear simulation method for the 1 : 2 complexation.⁴¹ In the other case, the K_S values were estimated by the simulation for the 1 : 1 complexation.

Low temperature NMR measurements

The solution of host **1** complexes with metal cations was prepared by the treatment in a supersonic homogenizer of host **1** [²H]chloroform–[²H₂]dichloromethane ($v/v = 1 : 3$) solution containing an excess amount of metal salt. The decanted solutions were used for the NMR experiment. The initial concentration of the host was 1.63 mM. The concentration of the complex was estimated at about 1.6 mM because of the large association ability in the low-polar solvent. The probe of the NMR instrument was slowly refrigerated by liquid nitrogen until the temperature was low enough (*ca.* 180 K) to observe coalescence behavior. ¹H-NMR spectra were measured at each temperature with increases of 10 K. The activation free energy (ΔG_c^\ddagger) values for the apparent conformational changes were estimated by the Eyring equation from the coalescence temperature (T_c) and the splitting width ($\Delta\nu$) of their proton peaks (3–5 peaks).

ESIMS experiments

ESIMS sample solutions were prepared by the following procedure. 10 μL of a 0.5 mM acetone solution of the host and 10 μL each of 5 mM acetone solutions of two different metal thiocyanates were mixed and diluted to 50 μL by adding acetone. The concentration of the host and two metal cations were 0.10, 1.0 and 1.0 mM. In all samples, potassium thiocyanate was used as the second metal salt for comparison. To maintain congruence between the peak intensity of the host **1**-metal complex ion and host **2**-metal complex ion, the relative peak intensity of the host **2**-metal complex ion was corrected by the relative peak intensity [$I(\text{host } \mathbf{2}\cdot\mathbf{K}^+)/I(\text{host } \mathbf{1}\cdot\mathbf{K}^+) = 0.11$] estimated from an ESI mass spectrum of a three component sample including hosts **1**, **2** and potassium thiocyanate.

ESI mass spectra were measured under the following conditions: syringe pump rate, 5 mL min^{-1} ; mass range, m/z 0–2000; capillary temperature, 150 °C; spray interface voltage, 4.50 kV; skimmer pump, 740 mTorr; scan time, 10 s; accumulation times, 10 scans. The sample solution was directly infused into an ion source.

Acknowledgements

We are very grateful to Mitsubishi Kagaku Co. for the kind donation of the cyclofructan mixture ($n = 6$ –8), to Professor Emeritus Takao Uchiyama (Osaka Kyuiku University) for his kind advice, to Dr Zenzaburo Totsuka, Mr Koji Matsuda, and Mr Yasuhiro Yamato (Fujisawa Pharm. Co.) for measurements of the ESI mass spectra, to Mr Hitoshi Yamada (ISIR, Osaka University) for the FABMS measurements, to Mrs Fusako Fukuda (ISIR) for elemental analyses, to Professors Takahiro Kaneda and Yoshiteru Sakata (ISIR) for permission to use the preparative gel-permeation liquid chromatography instrument in the early stage of our works, to Dr Shingo Yamamura (OMTRI) for the ion chromatographic analyses and atomic absorption analyses and to Dr Masaya Takahashi (OMTRI) for the solid NMR measurements.

References

- 1 B. C. Pressman, E. J. Harris, W. S. Jagger and J. H. Johnson, *Proc. Natl. Acad. Sci. USA*, 1967, **58**, 1949.
- 2 A. Agtarap, J. W. Chamberlin, M. Pinkerton and L. K. Steinrauf, *J. Am. Chem. Soc.*, 1967, **89**, 5737.
- 3 (a) B. C. Pressman, *Fed. Proc.*, 1968, **27**, 1283; (b) B. C. Pressman, *Annu. Rev. Biochem.*, 1976, **45**, 501.

- 4 (a) M. Noda, S. Shimizu, T. Tanabe, T. Takai, T. Kayano, T. Ikeda, H. Takahashi, H. Nakayama, Y. Kanaoka, N. Minamino, K. Kangawa, H. Matsuo, M. A. Raftery, T. Hirose, M. Notake, S. Inayama, H. Hayashida, T. Miyata and S. Numa, *Nature*, 1984, **312**, 121; (b) T. Tanabe, M. Takeshima, A. Mikami, V. Flockerzi, H. Takahashi, K. Kangawa, M. Kojima, H. Matsuo, T. Hirose and S. Numa, *Nature*, 1987, **328**, 313.
- 5 (a) C. J. Pedersen, *J. Am. Chem. Soc.*, 1967, **89**, 2495; (b) D. J. Cram, *Angew. Chem., Int. Ed. Engl.*, 1988, **27**, 1009.
- 6 (a) B. Dietrich, J.-M. Lehn and J. P. Sauvage, *Tetrahedron Lett.*, 1969, 2885; (b) J.-M. Lehn, *Angew. Chem., Int. Ed. Engl.*, 1988, **27**, 90.
- 7 D. J. Cram, T. Kaneda, R. C. Helgeson and G. M. Lein, *J. Am. Chem. Soc.*, 1979, **101**, 6752.
- 8 D. J. Cram, *Science*, 1983, **219**, 1177.
- 9 (a) C. D. Gutche and R. Muthukrishnan, *J. Org. Chem.*, 1978, **43**, 4905; (b) C. D. Gutche, B. Dhawan, K. H. No and R. Muthukrishnan, *J. Am. Chem. Soc.*, 1981, **103**, 3782; (c) S. Shinkai, K. Araki and O. Manabe, *J. Am. Chem. Soc.*, 1988, **110**, 7214.
- 10 A. F. Danil de Namor, R. M. Cleverley and M. L. Zapata-Ormachea, *Chem. Rev.*, 1998, **98**, 2495.
- 11 (a) M. Kawamura, T. Uchiyama, T. Kuramoto, Y. Tamura and K. Mizutani, *Carbohydr. Res.*, 1989, **192**, 83; (b) M. Kawamura and T. Uchiyama, *Carbohydr. Res.*, 1994, **260**, 297.
- 12 M. Sawada, T. Tanaka, Y. Takai, T. Hanafusa, T. Taniguchi, M. Kawamura and T. Uchiyama, *Carbohydr. Res.*, 1991, **217**, 7.
- 13 (a) T. Uchiyama, M. Kawamura, T. Uragami and H. Okuno, *Carbohydr. Res.*, 1993, **241**, 245; (b) N. Yoshie, H. Hamada, S. Takada and Y. Inoue, *Chem. Lett.*, 1993, 353.
- 14 (a) Y. Takai, Y. Okumura, S. Takahashi, M. Sawada, M. Kawamura and T. Uchiyama, *J. Chem. Soc., Chem. Commun.*, 1993, 53; (b) Y. Takai, Y. Okumura, M. Sawada, S. Takahashi, M. Siro, M. Kawamura and T. Uchiyama, *J. Org. Chem.*, 1994, **59**, 2967.
- 15 T. Kida, K. Isogawa, W. Zhang, Y. Nakatsuji and I. Ikeda, *Bull. Chem. Soc. Jpn.*, 1998, **71**, 1201.
- 16 (a) M. Bourgoin, K. H. Wong, J. Y. Hui and J. Smid, *J. Am. Chem. Soc.*, 1975, **97**, 3462; (b) A. Arduini, A. Pochini, S. Reverberi, R. Ungaro, G. D. Andreetti and F. Ugozzoli, *Tetrahedron*, 1986, **42**, 2089.
- 17 T. Arimura, M. Kubota, T. Matsuda, O. Manabe and S. Shinkai, *Bull. Chem. Soc. Jpn.*, 1989, **62**, 1674.
- 18 Y. Takeda and O. Arima, *Bull. Chem. Soc. Jpn.*, 1985, **58**, 3403.
- 19 M. Ohki, in *Applications of Dynamic NMR Spectroscopy to Organic Chemistry*, VCH Publishers, Inc., Weinheim, 1985, chapter 3, p. 11.
- 20 The conformation of the crown ether is mainly represented by the arrangement of the –O–C–O– torsion angles: $g^+ = \sim 0$ to $+120^\circ$, $g^- = 0$ to -120° , and $t = -120$ to 180° .
- 21 Space group: $1 \cdot K^+$ (Pic^-) complex, $P4_32_12$; $1 \cdot Rb^+$ (Pic^-) complex, $P4_12_12$; $1 \cdot Cs^+$ (Pic^-) complex, $P4_12_12$.
- 22 J. J. P. Stewart, *J. Comput. Chem.*, 1989, **10**, 209.
- 23 J. A. Pople and D. L. Beveridge, in *Approximate Molecular Orbital Theory*, McGraw-Hill Book Company, New York, 1970.
- 24 R. M. Izatt, K. Pawlak and J. S. Bradshaw, *Chem. Rev.*, 1991, **91**, 1721.
- 25 J. J. Christensen, D. J. Eatough and R. M. Izatt, *Chem. Rev.*, 1974, **74**, 351.
- 26 Y. Marcus, in *Ion Solvation*, John Wiley, New York, 1985.
- 27 R. D. Boss and A. I. Popov, *Inorg. Chem.*, 1986, **25**, 1747.
- 28 J. D. Dunitz, M. Dobler, P. Seiler and R. P. Phizackerley, *Acta Crystallogr., Sect. B*, 1974, **30**, 2733.
- 29 M. Dobler, J. D. Dunitz and P. Seiler, *Acta Crystallogr., Sect. B*, 1974, **30**, 2741.
- 30 S. Immel and F. W. Lichtenthaler, *Liebigs. Ann. Chem.*, 1996, 39.
- 31 (a) E. Leize, A. Jaffrezic and A. V. Dorselaer, *J. Mass Spectrom.*, 1996, **31**, 537; (b) S. M. Blair, E. C. Kempen and J. S. Brodbelt, *J. Am. Soc. Mass Spectrom.*, 1998, **9**, 1049; (c) K. Wang and G. W. Gokel, *J. Org. Chem.*, 1996, **61**, 4693.
- 32 M. Goodall, P. M. Kelly, D. Parker, K. Gloe and H. Stephan, *J. Chem. Soc., Perkin Trans. 2*, 1997, 59.
- 33 M. Sawada, Y. Takai, H. Yamada, J. Nishida, T. Kaneda, R. Arakawa, M. Okamoto, K. Hirose, T. Tanaka and K. Naemura, *J. Chem. Soc., Perkin Trans. 2*, 1998, 701.
- 34 (a) M. Yamashita and J. B. Fenn, *J. Phys. Chem.*, 1984, **88**, 4511; (b) M. Yamashita and J. B. Fenn, *J. Phys. Chem.*, 1984, **88**, 4671; (c) P. Kebarle and L. Tang, *Anal. Chem.*, 1993, **65**, 972A.
- 35 For example, D. Live and S. I. Chan, *J. Am. Chem. Soc.*, 1976, **98**, 3769.
- 36 M. Sawada, M. Shizuma, H. Adachi, Y. Takai, T. Takeda and T. Uchiyama, *Chem. Commun.*, 1998, 1453.
- 37 S. Hakomori, *J. Biochem. (Tokyo)*, 1964, **55**, 205.
- 38 M. A. McKervey, E. M. Seward, G. Ferguson, B. Ruhl and S. J. Harris, *J. Chem. Soc., Chem. Commun.*, 1985, 388.
- 39 M. A. Coplan and R. M. Fuoss, *J. Phys. Chem.*, 1964, **68**, 1177.
- 40 H. Tsukube and H. Sohmiya, *J. Org. Chem.*, 1991, **56**, 875.
- 41 R. P. Bonar-Law and J. K. M. Sanders, *J. Am. Chem. Soc.*, 1995, **117**, 259.